

# New paradigm for fluctuations in heavy-ion collisions

Giuliano Giacalone,<sup>1</sup> Pablo Guerrero-Rodríguez,<sup>2,3</sup> Matthew Luzum,<sup>4</sup> Cyrille Marquet,<sup>3</sup> and Jean-Yves Ollitrault<sup>1</sup>

<sup>1</sup>*Institut de physique théorique, Université Paris Saclay, CNRS, CEA, F-91191 Gif-sur-Yvette, France*

<sup>2</sup>*CAFPE and Departamento de Física Teórica y del Cosmos,*

*Universidad de Granada, E-18071 Campus de Fuentenueva, Granada, Spain*

<sup>3</sup>*CPHT, École Polytechnique, CNRS, Route de Saclay, 91128 Palaiseau, France*

<sup>4</sup>*Instituto de Física, Universidade de São Paulo, C.P. 66318, 05315-970 São Paulo, Brazil*

(Dated: February 20, 2019)

Since their discovery, fluctuations in the initial state of heavy-ion collisions have been understood as originating mostly from the random positions of nucleons within the colliding nuclei. We consider an alternative approach where all the focus is on fluctuations generated by QCD interactions, that we evaluate from first principles in the color glass condensate effective theory. Our approach provides an excellent description of RHIC and LHC data on anisotropic flow.

## INTRODUCTION

Relativistic heavy-ion collisions are performed at the BNL Relativistic Heavy Ion Collider (RHIC) and at the CERN Large Hadron Collider (LHC) with the aim of creating the quark-gluon plasma, the high-temperature state of strongly-interacting matter. The nuclear-sized droplet of quark-gluon plasma formed in a collision expands like a low-viscosity fluid [1], whose properties are studied through characteristic azimuthal anisotropies generated during the expansion [2–6]. In a hydrodynamic framework, azimuthal anisotropy in the final state is engendered by the spatial anisotropy that characterizes the energy-density profile at the onset of the hydrodynamic evolution [1, 7]. This *primordial* spatial anisotropy has, in a heavy-ion collision, a twofold origin: First, it is due to the almond shape of the overlap area between two nuclei for noncentral collisions, that generates elliptic flow [8]; Second, it originates from event-to-event density fluctuations [9], that yield an elliptic deformation even in central collisions [10], and a triangular anisotropy [11]. The role of primordial fluctuations for heavy-ion phenomenology draws, hence, an interesting parallel [12] with the physics of primordial fluctuations in cosmology, where the observed anisotropies of the Cosmic Microwave Background [13] originate from quantum fluctuations in the early Universe [14].

In the standard picture of heavy-ion collisions, primordial fluctuations originate from the randomness in the spatial positions of the nucleons that populate the wavefunctions of the colliding nuclei [15], with additional contributions at the level of the subnucleonic structure [16–18]. In addition, there are also fluctuations due to the collision process itself, i.e., to the gluon dynamics [19]. Putting all these effects together typically results in complex, fully numerical descriptions of the initial state [20–22] that do not offer an intuitive grasp of the relevant scales and phenomena.

In this paper, we achieve a more transparent description of initial-state fluctuations by applying a recent an-

alytical calculation of energy-density fluctuations [23] to the phenomenology of anisotropic flow in nucleus-nucleus collisions. Denoting by  $\rho(\mathbf{s})$ , where  $\mathbf{s}$  labels a point in the transverse plane, the energy density deposited at mid-rapidity right after a collision takes place, we write that  $\rho(\mathbf{s}) = \langle \rho(\mathbf{s}) \rangle + \delta\rho(\mathbf{s})$ , where  $\langle \rho(\mathbf{s}) \rangle$  is the energy density averaged over many events at a given impact parameter, and  $\delta\rho(\mathbf{s})$  is referred to as the fluctuation. Doing so, the magnitude of density fluctuations, which is given by their variance, or connected two-point function, is:

$$\begin{aligned} S(\mathbf{s}_1, \mathbf{s}_2) &\equiv \langle \delta\rho(\mathbf{s}_1)\delta\rho(\mathbf{s}_2) \rangle \\ &= \langle \rho(\mathbf{s}_1)\rho(\mathbf{s}_2) \rangle - \langle \rho(\mathbf{s}_1) \rangle \langle \rho(\mathbf{s}_2) \rangle. \end{aligned} \quad (1)$$

Albacete *et al.* [23] have calculated  $S(\mathbf{s}_1, \mathbf{s}_2)$  in the color glass condensate [24–26] (CGC) effective field theory of QCD. They have expressed  $S(\mathbf{s}_1, \mathbf{s}_2)$  analytically as a function of the saturation scales of the two nuclei and of the relative transverse distance  $r \equiv |\mathbf{s}_1 - \mathbf{s}_2|$ .

## INITIAL-STATE ANISOTROPIES FROM THE 2-POINT FUNCTION

The relevant quantities for phenomenology are dimensionless complex Fourier coefficients that characterize the spatial anisotropy of the initial density field,  $\rho(\mathbf{s})$ . They are defined, in a centered coordinate system<sup>1</sup>, as [27, 28]

$$\varepsilon_n \equiv \frac{\int_{\mathbf{s}} \mathbf{s}^n \rho(\mathbf{s})}{\int_{\mathbf{s}} |\mathbf{s}|^n \rho(\mathbf{s})}, \quad (2)$$

where we use the complex coordinate  $\mathbf{s} = x + iy$ , and the short hand  $\int_{\mathbf{s}} = \int dx dy$  for the integration over the transverse plane.  $\varepsilon_2$  and  $\varepsilon_3$  thus defined quantify, respectively, the amount of elliptic and triangular deformation of the density profile.

The coefficient of anisotropic flow,  $v_n$ , is defined as the  $n$ -th Fourier harmonic of the azimuthal distribution

---

<sup>1</sup> We mean that the center of energy lies at the origin,  $\int_{\mathbf{s}} \mathbf{s} \rho(\mathbf{s}) = 0$ .

of outgoing particles [29]. The largest harmonics in the spectrum are elliptic flow,  $v_2$ , and triangular flow,  $v_3$ . Hydrodynamic simulations show that for both of them,  $v_n$  is to a good approximation [30–32] proportional to  $\varepsilon_n$ , that is,  $v_n = \kappa_n \varepsilon_n$ , where  $\kappa_n$  is a hydrodynamic response coefficient which depends mildly on the impact parameter of the collision for a given colliding system and energy.

Anisotropic flow is not measured on an event-by-event basis, but inferred from correlations which are averaged over events in a given class of collision centrality. The default measure of  $v_n$  is an rms average, denoted by  $v_n\{2\} \equiv \langle |v_n|^2 \rangle^{1/2}$  [33], where the 2 inside curly brackets means that it is inferred from analyses of 2-particle correlations. Linear response implies  $v_n\{2\} = \kappa_n \varepsilon_n\{2\}$ . Thus, the relevant quantity from the initial state is the rms average of  $\varepsilon_n$ , denoted by  $\varepsilon_n\{2\}$ . It turns out that this quantity can be expressed in terms of the two-point function,  $S(\mathbf{s}_1, \mathbf{s}_2)$ , under fairly general assumptions [34].

Let us start with the simple case of a collision at zero impact parameter. Since the mean density profile,  $\langle \rho(\mathbf{s}) \rangle$ , is azimuthally symmetric, one can replace  $\rho(\mathbf{s})$  with  $\delta\rho(\mathbf{s})$  in the numerator of Eq. (2). To leading order in the fluctuation,  $\delta\rho(\mathbf{s})$ , then, one can replace  $\rho(\mathbf{s})$  with  $\langle \rho(\mathbf{s}) \rangle$  in the denominator. Multiplying by the complex conjugate,  $\varepsilon_n^*$ , and averaging over events, one immediately obtains [34]:

$$\varepsilon_n\{2\}^2 \equiv \langle |\varepsilon_n|^2 \rangle = \frac{\int_{\mathbf{s}_1, \mathbf{s}_2} (\mathbf{s}_1)^n (\mathbf{s}_2^*)^n S(\mathbf{s}_1, \mathbf{s}_2)}{\left( \int_{\mathbf{s}} |\mathbf{s}|^n \langle \rho(\mathbf{s}) \rangle \right)^2}. \quad (3)$$

We now generalize to non-central collisions. The main difference is that the mean density profile,  $\langle \rho(\mathbf{s}) \rangle$ , is no longer isotropic, but has an elliptic shape. Its departure from isotropy is quantified by the mean anisotropy  $\bar{\varepsilon}_2$ , which is given by replacing  $\rho(\mathbf{s})$  with  $\langle \rho(\mathbf{s}) \rangle$  in Eq. (2):

$$\bar{\varepsilon}_2 \equiv \frac{\int_{\mathbf{s}} \mathbf{s}^2 \langle \rho(\mathbf{s}) \rangle}{\int_{\mathbf{s}} |\mathbf{s}|^2 \langle \rho(\mathbf{s}) \rangle}. \quad (4)$$

This is a quantity of direct phenomenological relevance. Indeed, the fourth-cumulant measure of elliptic flow,  $v_2\{4\} \equiv (2\langle v_2^2 \rangle^2 - \langle v_n^4 \rangle)^{1/4}$  [35], is, in the regime of linear hydrodynamic response, equal to  $v_2\{4\} = \kappa_2 \varepsilon_2\{4\}$ , where  $\varepsilon_2\{4\}$  is the fourth-order cumulant of  $\varepsilon_2$  fluctuations, that can be taken as:

$$\varepsilon_2\{4\} \approx \bar{\varepsilon}_2. \quad (5)$$

Equation (5) assumes that  $\bar{\varepsilon}_2$  coincides with the mean eccentricity in the reaction plane [36] and that eccentricity fluctuations are Gaussian [37, 38]. This turns out to be a very good approximation for collisions up to  $\sim 30\%$  centrality, after which non-Gaussian correction become sizable [39–43].

The total rms eccentricity,  $\varepsilon_2\{2\}$ , is obtained by adding in quadrature the mean eccentricity and the contribution of fluctuations, which is the right-hand side of Eq. (3).

Therefore, for non-central collisions, we simply replace Eq. (3) with

$$\sigma^2 \equiv \varepsilon_2\{2\}^2 - \bar{\varepsilon}_2^2 = \frac{\int_{\mathbf{s}_1, \mathbf{s}_2} (\mathbf{s}_1)^2 (\mathbf{s}_2^*)^2 S(\mathbf{s}_1, \mathbf{s}_2)}{\left( \int_{\mathbf{s}} |\mathbf{s}|^2 \langle \rho(\mathbf{s}) \rangle \right)^2}$$

$$\varepsilon_3\{2\}^2 = \frac{\int_{\mathbf{s}_1, \mathbf{s}_2} (\mathbf{s}_1)^3 (\mathbf{s}_2^*)^3 S(\mathbf{s}_1, \mathbf{s}_2)}{\left( \int_{\mathbf{s}} |\mathbf{s}|^3 \langle \rho(\mathbf{s}) \rangle \right)^2}, \quad (6)$$

where we introduce the notation  $\sigma^2$  for the variance of  $\varepsilon_2$  fluctuations. Corrections from recentering and energy conservation modify Eq. (6) for non-central collisions [36, 44], but we have checked numerically that such contributions are negligible.

## 1- AND 2-POINT FUNCTIONS FROM THE CGC

Derivations of the initial average energy density,  $\langle \rho(\mathbf{s}) \rangle$ , in the CGC framework date back to several years [45, 46]. Following Ref. [23], with  $N_c = 3$ , it simply reads:

$$\langle \rho(\mathbf{s}) \rangle = \frac{4}{3g^2} Q_A^2(\mathbf{s}) Q_B^2(\mathbf{s}), \quad (7)$$

where subscripts  $A$  and  $B$  label the two colliding nuclei,  $g$  is the strong coupling constant, and  $Q_{A,B}(\mathbf{s})$  is the local saturation scale of the nucleus.  $Q_A^2(\mathbf{s})$  is proportional to the density of nucleons per transverse area at point  $\mathbf{s}$ , which is traditionally denoted by  $T_A(\mathbf{s})$ , and is obtained by integrating the nuclear density over the longitudinal coordinate [15].

To the extent that the nuclear density is known, one obtains a parameter-free prediction for the mean eccentricity [47]:

$$\bar{\varepsilon}_2 \equiv \frac{\int_{\mathbf{s}} \mathbf{s}^2 T_A(\mathbf{s}) T_B(\mathbf{s})}{\int_{\mathbf{s}} |\mathbf{s}|^2 T_A(\mathbf{s}) T_B(\mathbf{s})}. \quad (8)$$

Figure 1(a) displays  $|\bar{\varepsilon}_2|$  defined by Eq. (8) as a function of impact parameter for a Pb+Pb collision. It is natural to ask whether this calculation is able to match the results of a state-of-the-art Monte Carlo model of nucleus-nucleus collisions, such as the IP Glasma model [21]. To this purpose, we compare our result with the value of  $|\bar{\varepsilon}_2|$  given by the TRENTo model [48] tuned as in Ref. [49], that enables one to accurately reproduce the multiplicity distributions and the cumulants of  $v_n$  fluctuations measured at the LHC, as well as the anisotropies of IP Glasma. We find that the TRENTo and the CGC results are almost identical.

The crucial new information coming from the CGC theory is the two-point function,  $S(\mathbf{s}_1, \mathbf{s}_2)$ , computed in Ref. [23], which allows us to evaluate  $\varepsilon_2\{2\}$  and  $\varepsilon_3\{2\}$ , as given by Eq. (6). The CGC typically predicts that the energy-density fluctuations are correlated over a transverse extent of order  $1/Q_s$  [50], which is much shorter than the nuclear radius,  $R$ . In other terms,  $S(\mathbf{s}_1, \mathbf{s}_2)$  is

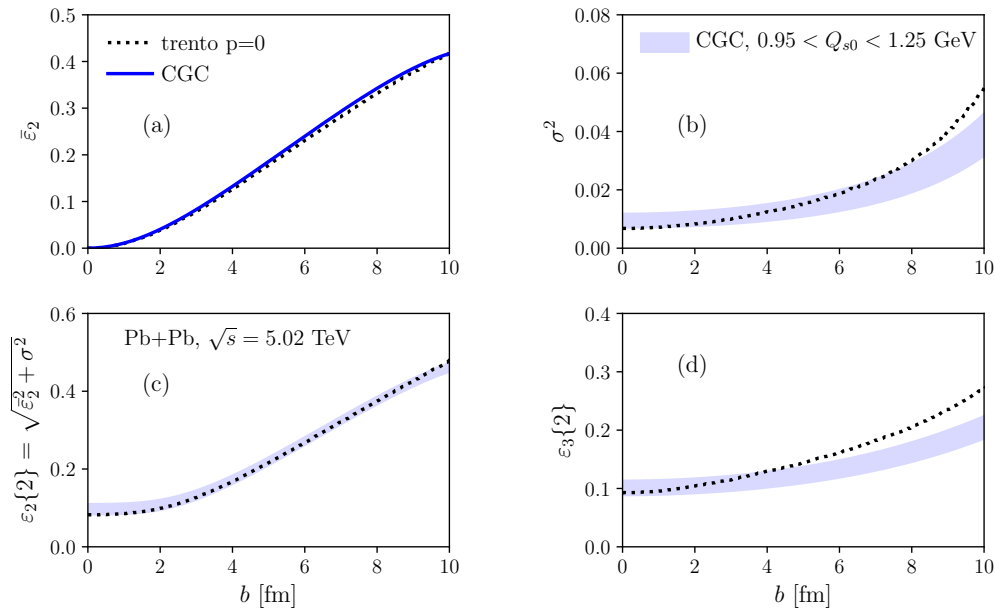


FIG. 1. Anisotropy fluctuations as function of impact parameter in 5.02 TeV Pb+Pb collisions. Dotted lines: T<sub>RENT</sub>o model tuned to LHC data. The solid line in panel (a) corresponds to Eq. (8) while the shaded bands in panels (b), (c), and (d) correspond to Eqs. (11). The shaded bands represent the variation of  $Q_{s0}$ .

small if  $r = |\mathbf{s}_1 - \mathbf{s}_2| \gg 1/Q_s$ . Therefore, it is natural to change variables to  $\mathbf{s}_1 = \mathbf{s} + \mathbf{r}/2$ ,  $\mathbf{s}_2 = \mathbf{s} - \mathbf{r}/2$ , and integrate first over  $\mathbf{r}$ . Albacete *et al.* show that  $S(\mathbf{s} + \mathbf{r}/2, \mathbf{s} - \mathbf{r}/2)$  falls off slowly at large distances, like  $1/r^2$ , so that the integral is logarithmically divergent. It must be regulated by an infrared cutoff,  $m$ , corresponding typically to a confinement scale, for which we choose

the pion mass,  $m = 0.14$  GeV.

Hence, with the following separation of scales in the system

$$\frac{1}{Q_s} \ll \frac{1}{m} \ll R \quad (9)$$

one can take  $S(\mathbf{s}_1, \mathbf{s}_2)$  from Ref. [23], whose integral over  $\mathbf{r}$  yields:<sup>2</sup>

$$\xi(\mathbf{s}) \equiv \int_{\mathbf{r}} S\left(\mathbf{s} + \frac{\mathbf{r}}{2}, \mathbf{s} - \frac{\mathbf{r}}{2}\right) = \frac{16\pi}{9g^4} Q_A^2(\mathbf{s}) Q_B^2(\mathbf{s}) \left( Q_A^2(\mathbf{s}) \ln\left(\frac{Q_B^2(\mathbf{s})}{m^2}\right) + Q_B^2(\mathbf{s}) \ln\left(\frac{Q_A^2(\mathbf{s})}{m^2}\right) \right), \quad (10)$$

where we keep only the logarithmically enhanced terms. Equations (6) then give [34]:

$$\begin{aligned} \sigma^2 &= \varepsilon_2\{2\}^2 - \bar{\varepsilon}_2^2 = \frac{\int_{\mathbf{s}} |\mathbf{s}|^4 \xi(\mathbf{s})}{\left(\int_{\mathbf{s}} |\mathbf{s}|^2 \langle \rho(\mathbf{s}) \rangle\right)^2} \\ \varepsilon_3\{2\}^2 &= \frac{\int_{\mathbf{s}} |\mathbf{s}|^6 \xi(\mathbf{s})}{\left(\int_{\mathbf{s}} |\mathbf{s}|^3 \langle \rho(\mathbf{s}) \rangle\right)^2}, \end{aligned} \quad (11)$$

where we used the approximation that the range of correlation is much smaller than the nuclear radius.

Inserting Eqs. (7) and (10) into Eqs. (11), one sees that the coupling constant,  $g$ , cancels between the numerator and the denominator. Thus, the only free parameter in our calculation is the proportionality constant between  $(Q_A)^2$  and  $T_A$ , or, equivalently, the value of  $Q_A$  at the center of the nucleus, which we denote by  $Q_{s0}$ .

Finally, with Eqs. (11) at hand, it is important to observe how eccentricity fluctuations in our CGC picture compare to a state-of-the-art Monte Carlo model, where  $\varepsilon_n$  fluctuations are mostly due to fluctuating positions of nucleons. Again, we compare our results to the previous T<sub>RENT</sub>o calculation tuned to LHC data. Results from T<sub>RENT</sub>o are shown as dotted lines in Fig. 1 (b), (c), (d). The CGC result from Eq. (11) is shown as a shaded band corresponding to a range of  $Q_{s0}$  around 1.1 GeV. CGC

<sup>2</sup> We use the MV model expression of Ref. [23], and neglect the  $\alpha_s \ln(Q/m)$  dependence of the saturation scales, where  $Q$  corresponds either to a UV cutoff or to  $1/r$ .

and T<sub>RENT</sub>o give similar results. For both models, fluctuations (as measured by  $\sigma^2$  and  $\varepsilon_3\{2\}$  in panels (b) and (d)) increase as a function of impact parameter, which is understood as a natural consequence of the smaller system size. However, a closer examination reveals that the increase is milder in our CGC calculation.

Note that the CGC framework uses expressions for  $\langle\rho(\mathbf{s})\rangle$  and  $S(\mathbf{s}_1, \mathbf{s}_2)$  that describe the system right after the collision takes place, whereas T<sub>RENT</sub>o gives the entropy profile of the system at the beginning of hydrodynamics. This difference is not important, as classical Yang-Mills evolution to a finite proper time does not modify the eccentricity harmonics [51].

## COMPARISON WITH RHIC AND LHC DATA

We now compare our CGC calculations to experimental data on  $v_2\{2\}$ ,  $v_2\{4\}$  and  $v_3\{2\}$  in Pb+Pb collisions at  $\sqrt{s_{\text{NN}}} = 5.02$  TeV [41], and in Au+Au collisions at  $\sqrt{s_{\text{NN}}} = 200$  GeV [52]. Linear hydrodynamic response implies the following relations between final-state flow harmonics and initial-state anisotropies:

$$\begin{aligned} v_2\{2\} &= \kappa_2 \varepsilon_2\{2\}, \\ v_2\{4\} &= \kappa_2 \bar{\varepsilon}_2, \\ v_3\{2\} &= \kappa_3 \varepsilon_3\{2\}. \end{aligned} \quad (12)$$

We treat  $\kappa_2$ ,  $\kappa_3$ , and  $Q_{s0}$  as free parameters which we adjust to data. We restrict our theory-to-data comparison to the 0-30% centrality range, in which  $\kappa_n$  is essentially constant in hydrodynamics [53]. We use the geometric relation between the impact parameter and the centrality of a collision to express our results as function of the centrality percentile, i.e., we use  $centrality = (\pi b^2)/\sigma_{\text{inel}}$ , where  $\sigma_{\text{inel}}$  is the inelastic nucleus-nucleus cross section, which we take from the Glauber model:  $\sigma_{\text{inel}} = 685$  fm<sup>2</sup> in Au+Au collisions, and  $\sigma_{\text{inel}} = 777$  fm<sup>2</sup> in Pb+Pb collisions. We now explain how the values of  $\kappa_2$ ,  $\kappa_3$ , and  $Q_{s0}$  are chosen.

Since the mean eccentricity in the reaction plane,  $\bar{\varepsilon}_2$ , in Eqs. (8) does not depend on  $Q_{s0}$ , we first use  $v_2\{4\}$  to fix the value of  $\kappa_2$ . Figure 2 shows that with a single rescaling factor, we are able to reproduce the measured centrality dependence of  $v_2\{4\}$ , both at RHIC and at LHC.<sup>3</sup>

With the knowledge of  $\kappa_2$  at hand, we move on to the description of  $v_2\{2\} = \kappa_2 \varepsilon_2\{2\}$ . This quantity is less trivial because it depends on  $Q_{s0}$ . The gray shaded bands in Fig. 2 show the rescaled  $\varepsilon_2\{2\}$  corresponding to a range of values of  $Q_{s0}$ , in excellent agreement with  $v_2\{2\}$  data.

As expected from Fig. 1, LHC data [panel (a)] are reproduced in our calculation with a value of  $Q_{s0}$  of order 1.1 GeV. At RHIC energies [panel (b)], on the other hand, we find that  $Q_{s0}$  is lower, of order 0.7 GeV. This increase of  $Q_{s0}$  by factor 1.6 from RHIC to LHC is precisely that expected in the CGC picture, where  $Q_s^2 \propto \sqrt{s}^\lambda$ , with  $\lambda \sim 0.28$  [26], which gives a factor 1.6 from 200 GeV to 5.02 TeV. This energy dependence of fluctuations allows the CGC formalism to capture very transparently the nontrivial observation that the splitting between  $v_2\{2\}$  and  $v_2\{4\}$  is larger at RHIC than at LHC.

Finally, we fit the value of  $\kappa_3$  to match the value of  $v_3\{2\}$  in central collisions. Agreement with data is excellent throughout the chosen centrality range. Note that it would not be as good with the T<sub>RENT</sub>o model, which predicts a steeper increase of  $\varepsilon_3\{2\}$  with the centrality.

## DISCUSSION AND OUTLOOK

We have shown that energy fluctuations calculated in the CGC effective theory yield initial anisotropies which match values of  $v_2\{2\}$ ,  $v_2\{4\}$  and  $v_3\{2\}$  measured in central to midcentral nucleus-nucleus collisions at RHIC and LHC. Note that this is obtained for values of  $\kappa_2$  and  $\kappa_3$  that are very reasonable, in the sense that they are compatible with those found in state-of-the-art viscous hydrodynamic calculations [53].

Usual approaches to initial-state fluctuations start with a Monte Carlo Glauber calculation, which is used to sample the position of nucleons within nuclei. We now briefly argue that this stage of the calculation should be bypassed in modeling initial-state fluctuations.

The picture of the nucleus returned by the Monte Carlo Glauber simulation is essentially that of an ideal gas of pointlike particles [36], in the sense that correlations between nucleons have a negligible effect [55, 56] and that observables are insensitive to the size of initial inhomogeneities [57]. In other terms, if one replaces  $\rho(\mathbf{s})$  in Eq. (1) with the transverse density of participant nucleons, the two point function  $S(\mathbf{s}_1, \mathbf{s}_2)$  is proportional to  $\delta(\mathbf{s}_1 - \mathbf{s}_2)$ , and the proportionality factor is the mean density of nucleons per transverse area as evaluated in an optical Glauber model,  $\langle\rho(\mathbf{s})\rangle \sim T_A(\mathbf{s}) + T_B(\mathbf{s})$ .

This is reminiscent of the McLerran-Venugopalan model [58] which lies at the root of the CGC effective theory. One assumes that the color fields are generated by pointlike, independent color charges whose two-point function is proportional to  $\delta(\mathbf{s}_1 - \mathbf{s}_2)$ , where the proportionality factor is proportional to the nuclear thickness function  $T_A(\mathbf{s})$ . Therefore, the pointlike constituents of the Glauber model are already implicitly present in the CGC effective theory. Sampling the positions of nucleons and giving them a transverse extension [59] prior to evaluating locally the saturation scale, as is done in the IP Glasma approach [21, 60], implies a double counting

<sup>3</sup> The sharp decrease of  $v_2\{4\}$  at RHIC below 5% centrality is an effect of centrality fluctuations [54], which are not included in our description.

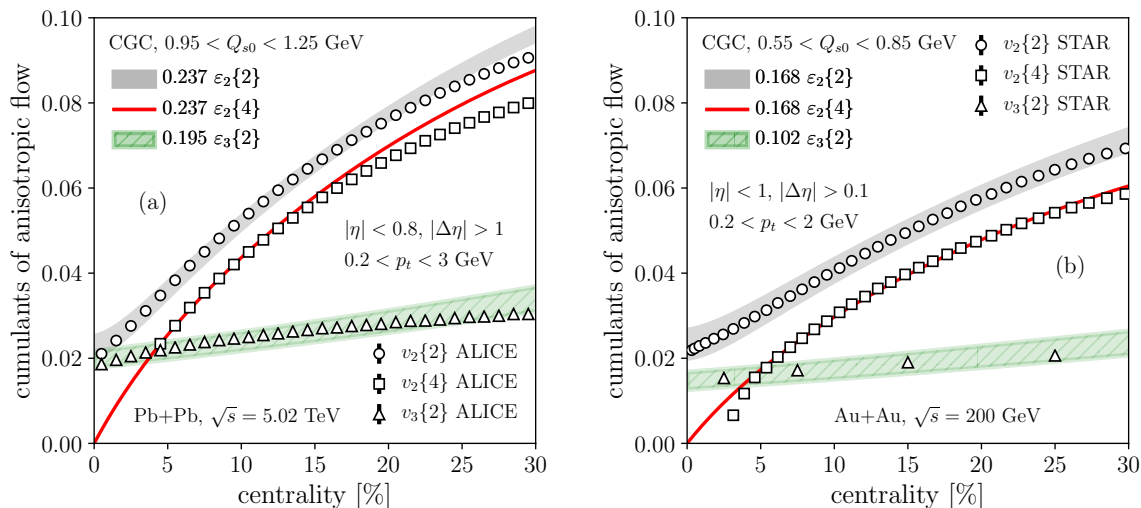


FIG. 2. Symbols: Experimental data on  $v_2$  and  $v_3$ , as function of centrality percentile, measured by the ALICE Collaboration in 5.02 TeV Pb+Pb collisions [panel (a)], and by the STAR Collaboration in 200 GeV Au+Au collisions [panel (b)]. Lines and shaded bands represent results from our CGC formalism, rescaled according to Eq. (12). The shaded bands indicate a variation in the value of  $Q_{s0}$ .

of the relevant fluctuations.

Note that the CGC calculation of fluctuations, unlike the Monte Carlo Glauber model, does not boil down to an ideal gas of identical, pointlike sources. The statistics of density fluctuations in an ideal gas follows Poisson statistics, with a variance proportional to the mean. By contrast, in the CGC picture, the mean is proportional to  $Q_s^4$  [Eq. (7)], while the variance is proportional to  $Q_s^6$  [Eq. (10)], neglecting the smoothly-varying logarithm. This enhances the role of fluctuations at the center of the fireball. The phenomenological consequences of this prediction of high-energy QCD, which follows essentially from dimensional analysis, deserve further investigations.

### ACKNOWLEDGEMENTS

J-Y.O. thanks Jean-Paul Blaizot, Wojciech Broniowski, François Gelis, Dong Jo Kim, Tuomas Lappi, Aleksas Mazeliauskas for discussions. M.L. acknowledges support from FAPESP projects 2016/24029-6 and 2017/05685-2, and project INCT-FNA Proc. No. 464898/2014-5. M.L. and G.G. acknowledge funding from the USP-COFEUCUB project Uc Ph 160-16 (2015/13). P.G-R. acknowledges financial support from the ‘La Caixa’ Banking Foundation. The work of CM was supported in part by the Agence Nationale de la Recherche under the project ANR-16-CE31-0019-02.

[1] U. Heinz and R. Snellings, *Ann. Rev. Nucl. Part. Sci.* **63**, 123 (2013) doi:10.1146/annurev-nucl-102212-170540

[arXiv:1301.2826 [nucl-th]].  
 [2] J. Adams *et al.* [STAR Collaboration], *Phys. Rev. C* **72**, 014904 (2005) doi:10.1103/PhysRevC.72.014904 [nucl-ex/0409033].  
 [3] S. S. Adler *et al.* [PHENIX Collaboration], *Phys. Rev. Lett.* **91**, 182301 (2003) doi:10.1103/PhysRevLett.91.182301 [nucl-ex/0305013].  
 [4] K. Aamodt *et al.* [ALICE Collaboration], *Phys. Rev. Lett.* **105**, 252302 (2010) doi:10.1103/PhysRevLett.105.252302 [arXiv:1011.3914 [nucl-ex]].  
 [5] G. Aad *et al.* [ATLAS Collaboration], *Phys. Rev. C* **86**, 014907 (2012) doi:10.1103/PhysRevC.86.014907 [arXiv:1203.3087 [hep-ex]].  
 [6] S. Chatrchyan *et al.* [CMS Collaboration], *Phys. Rev. C* **87**, no. 1, 014902 (2013) doi:10.1103/PhysRevC.87.014902 [arXiv:1204.1409 [nucl-ex]].  
 [7] L. Yan, *Chin. Phys. C* **42**, no. 4, 042001 (2018) doi:10.1088/1674-1137/42/4/042001 [arXiv:1712.04580 [nucl-th]].  
 [8] J. Y. Ollitrault, *Phys. Rev. D* **46**, 229 (1992). doi:10.1103/PhysRevD.46.229  
 [9] M. Miller and R. Snellings, nucl-ex/0312008.  
 [10] B. Alver *et al.* [PHOBOS Collaboration], *Phys. Rev. Lett.* **98**, 242302 (2007) doi:10.1103/PhysRevLett.98.242302 [nucl-ex/0610037].  
 [11] B. Alver and G. Roland, *Phys. Rev. C* **81**, 054905 (2010) Erratum: [Phys. Rev. C **82**, 039903 (2010)] doi:10.1103/PhysRevC.82.039903, 10.1103/PhysRevC.81.054905 [arXiv:1003.0194 [nucl-th]].  
 [12] A. P. Mishra, R. K. Mohapatra, P. S. Saumia and A. M. Srivastava, *Phys. Rev. C* **77**, 064902 (2008) doi:10.1103/PhysRevC.77.064902 [arXiv:0711.1323 [hep-ph]].  
 [13] P. A. R. Ade *et al.* [Planck Collaboration], *Astron. Astrophys.* **571**, A15 (2014) doi:10.1051/0004-6361/201321573 [arXiv:1303.5075 [astro-ph.CO]].

- [14] J. M. Bardeen, P. J. Steinhardt and M. S. Turner, Phys. Rev. D **28**, 679 (1983). doi:10.1103/PhysRevD.28.679
- [15] M. L. Miller, K. Reygers, S. J. Sanders and P. Steinberg, Ann. Rev. Nucl. Part. Sci. **57**, 205 (2007) doi:10.1146/annurev.nucl.57.090506.123020 [nucl-ex/0701025].
- [16] S. Eremín and S. Voloshin, Phys. Rev. C **67**, 064905 (2003) doi:10.1103/PhysRevC.67.064905 [nucl-th/0302071].
- [17] A. Bialas and A. Bzdak, Phys. Lett. B **649**, 263 (2007) Erratum: [Phys. Lett. B **773**, 681 (2017)] doi:10.1016/j.physletb.2007.04.014, 10.1016/j.physletb.2017.10.007 [nucl-th/0611021].
- [18] C. Loizides, Phys. Rev. C **94**, no. 2, 024914 (2016) doi:10.1103/PhysRevC.94.024914 [arXiv:1603.07375 [nucl-ex]].
- [19] T. Lappi, Phys. Rev. C **67**, 054903 (2003) doi:10.1103/PhysRevC.67.054903 [hep-ph/0303076].
- [20] J. L. Albacete and A. Dumitru, arXiv:1011.5161 [hep-ph].
- [21] B. Schenke, P. Tribedy and R. Venugopalan, Phys. Rev. Lett. **108**, 252301 (2012) doi:10.1103/PhysRevLett.108.252301 [arXiv:1202.6646 [nucl-th]].
- [22] H. Niemi, K. J. Eskola and R. Paatelainen, Phys. Rev. C **93**, no. 2, 024907 (2016) doi:10.1103/PhysRevC.93.024907 [arXiv:1505.02677 [hep-ph]].
- [23] J. L. Albacete, P. Guerrero-Rodríguez and C. Marquet, JHEP **1901**, 073 (2019) doi:10.1007/JHEP01(2019)073 [arXiv:1808.00795 [hep-ph]].
- [24] E. Iancu, A. Leonidov and L. D. McLerran, Nucl. Phys. A **692**, 583 (2001) doi:10.1016/S0375-9474(01)00642-X [hep-ph/0011241].
- [25] F. Gelis, E. Iancu, J. Jalilian-Marian and R. Venugopalan, Ann. Rev. Nucl. Part. Sci. **60**, 463 (2010) doi:10.1146/annurev.nucl.010909.083629 [arXiv:1002.0333 [hep-ph]].
- [26] J. L. Albacete and C. Marquet, Prog. Part. Nucl. Phys. **76**, 1 (2014) doi:10.1016/j.ppnp.2014.01.004 [arXiv:1401.4866 [hep-ph]].
- [27] D. Teaney and L. Yan, Phys. Rev. C **83**, 064904 (2011) doi:10.1103/PhysRevC.83.064904 [arXiv:1010.1876 [nucl-th]].
- [28] Z. Qiu and U. W. Heinz, Phys. Rev. C **84**, 024911 (2011) doi:10.1103/PhysRevC.84.024911 [arXiv:1104.0650 [nucl-th]].
- [29] M. Luzum, J. Phys. G **38**, 124026 (2011) doi:10.1088/0954-3899/38/12/124026 [arXiv:1107.0592 [nucl-th]].
- [30] F. G. Gardim, F. Grassi, M. Luzum and J. Y. Ollitrault, Phys. Rev. C **85**, 024908 (2012) doi:10.1103/PhysRevC.85.024908 [arXiv:1111.6538 [nucl-th]].
- [31] H. Niemi, G. S. Denicol, H. Holopainen and P. Huovinen, Phys. Rev. C **87**, no. 5, 054901 (2013) doi:10.1103/PhysRevC.87.054901 [arXiv:1212.1008 [nucl-th]].
- [32] F. G. Gardim, J. Noronha-Hostler, M. Luzum and F. Grassi, Phys. Rev. C **91**, no. 3, 034902 (2015) doi:10.1103/PhysRevC.91.034902 [arXiv:1411.2574 [nucl-th]].
- [33] M. Luzum and J. Y. Ollitrault, Phys. Rev. C **87**, no. 4, 044907 (2013) doi:10.1103/PhysRevC.87.044907 [arXiv:1209.2323 [nucl-ex]].
- [34] J. P. Blaizot, W. Broniowski and J. Y. Ollitrault, Phys. Lett. B **738**, 166 (2014) doi:10.1016/j.physletb.2014.09.028 [arXiv:1405.3572 [nucl-th]].
- [35] N. Borghini, P. M. Dinh and J. Y. Ollitrault, Phys. Rev. C **64**, 054901 (2001) doi:10.1103/PhysRevC.64.054901 [nucl-th/0105040].
- [36] R. S. Bhalerao and J. Y. Ollitrault, Phys. Lett. B **641**, 260 (2006) doi:10.1016/j.physletb.2006.08.055 [nucl-th/0607009].
- [37] S. A. Voloshin, A. M. Poskanzer, A. Tang and G. Wang, Phys. Lett. B **659**, 537 (2008) doi:10.1016/j.physletb.2007.11.043 [arXiv:0708.0800 [nucl-th]].
- [38] S. Floerchinger and U. A. Wiedemann, JHEP **1408**, 005 (2014) doi:10.1007/JHEP08(2014)005 [arXiv:1405.4393 [hep-ph]].
- [39] G. Giacalone, L. Yan, J. Noronha-Hostler and J. Y. Ollitrault, Phys. Rev. C **95**, no. 1, 014913 (2017) doi:10.1103/PhysRevC.95.014913 [arXiv:1608.01823 [nucl-th]].
- [40] A. M. Sirunyan *et al.* [CMS Collaboration], Phys. Lett. B **789**, 643 (2019) doi:10.1016/j.physletb.2018.11.063 [arXiv:1711.05594 [nucl-ex]].
- [41] S. Acharya *et al.* [ALICE Collaboration], JHEP **1807**, 103 (2018) doi:10.1007/JHEP07(2018)103 [arXiv:1804.02944 [nucl-ex]].
- [42] H. Mehrappour and S. F. Taghavi, Eur. Phys. J. C **79**, no. 1, 88 (2019) doi:10.1140/epjc/s10052-019-6549-2 [arXiv:1805.04695 [nucl-th]].
- [43] R. S. Bhalerao, G. Giacalone and J. Y. Ollitrault, Phys. Rev. C **99**, no. 1, 014907 (2019) doi:10.1103/PhysRevC.99.014907 [arXiv:1811.00837 [nucl-th]].
- [44] R. S. Bhalerao, M. Luzum and J. Y. Ollitrault, Phys. Rev. C **84**, 054901 (2011) doi:10.1103/PhysRevC.84.054901 [arXiv:1107.5485 [nucl-th]].
- [45] T. Lappi, Phys. Lett. B **643**, 11 (2006) doi:10.1016/j.physletb.2006.10.017 [hep-ph/0606207].
- [46] G. Chen, R. J. Fries, J. I. Kapusta and Y. Li, Phys. Rev. C **92**, no. 6, 064912 (2015) doi:10.1103/PhysRevC.92.064912 [arXiv:1507.03524 [nucl-th]].
- [47] T. Lappi and R. Venugopalan, Phys. Rev. C **74**, 054905 (2006) doi:10.1103/PhysRevC.74.054905 [nucl-th/0609021].
- [48] J. S. Moreland, J. E. Bernhard and S. A. Bass, Phys. Rev. C **92**, no. 1, 011901 (2015) doi:10.1103/PhysRevC.92.011901 [arXiv:1412.4708 [nucl-th]].
- [49] G. Giacalone, J. Noronha-Hostler, M. Luzum and J. Y. Ollitrault, Phys. Rev. C **97**, no. 3, 034904 (2018) doi:10.1103/PhysRevC.97.034904 [arXiv:1711.08499 [nucl-th]].
- [50] T. Lappi, Phys. Lett. B **744**, 315 (2015) doi:10.1016/j.physletb.2015.04.015 [arXiv:1501.05505 [hep-ph]].
- [51] B. Schenke, P. Tribedy and R. Venugopalan, Phys. Rev. C **86**, 034908 (2012) doi:10.1103/PhysRevC.86.034908 [arXiv:1206.6805 [hep-ph]].
- [52] L. Adamczyk *et al.* [STAR Collaboration], Phys. Rev. Lett. **115**, no. 22, 222301 (2015)

- doi:10.1103/PhysRevLett.115.222301 [arXiv:1505.07812 [nucl-ex]].
- [53] J. Noronha-Hostler, L. Yan, F. G. Gardim and J. Y. Ollitrault, Phys. Rev. C **93**, no. 1, 014909 (2016) doi:10.1103/PhysRevC.93.014909 [arXiv:1511.03896 [nucl-th]].
- [54] M. Zhou and J. Jia, Phys. Rev. C **98**, no. 4, 044903 (2018) doi:10.1103/PhysRevC.98.044903 [arXiv:1803.01812 [nucl-th]].
- [55] M. Alvioli, H. Holopainen, K. J. Eskola and M. Strikman, Phys. Rev. C **85**, 034902 (2012) doi:10.1103/PhysRevC.85.034902 [arXiv:1112.5306 [hep-ph]].
- [56] J. P. Blaizot, W. Broniowski and J. Y. Ollitrault, Phys. Rev. C **90**, no. 3, 034906 (2014) doi:10.1103/PhysRevC.90.034906 [arXiv:1405.3274 [nucl-th]].
- [57] F. G. Gardim, F. Grassi, P. Ishida, M. Luzum, P. S. Magalhes and J. Noronha-Hostler, Phys. Rev. C **97**, no. 6, 064919 (2018) doi:10.1103/PhysRevC.97.064919 [arXiv:1712.03912 [nucl-th]].
- [58] L. D. McLerran and R. Venugopalan, Phys. Rev. D **49**, 2233 (1994) doi:10.1103/PhysRevD.49.2233 [hep-ph/9309289].
- [59] H. Kowalski and D. Teaney, Phys. Rev. D **68**, 114005 (2003) doi:10.1103/PhysRevD.68.114005 [hep-ph/0304189].
- [60] J. L. Nagle and W. A. Zajc, arXiv:1808.01276 [nucl-th].